LBNL-46695

ERNEST ORLANDO LAWRENCE
BERKELEY NATIONAL LABORATORY

Potential Impacts of Climate Change on Tropospheric Ozone in California: A Preliminary Episodic Modeling Assessment of the Los Angeles Basin and the Sacramento Valley

Haider Taha

Environmental Energy Technologies Division

January 2001

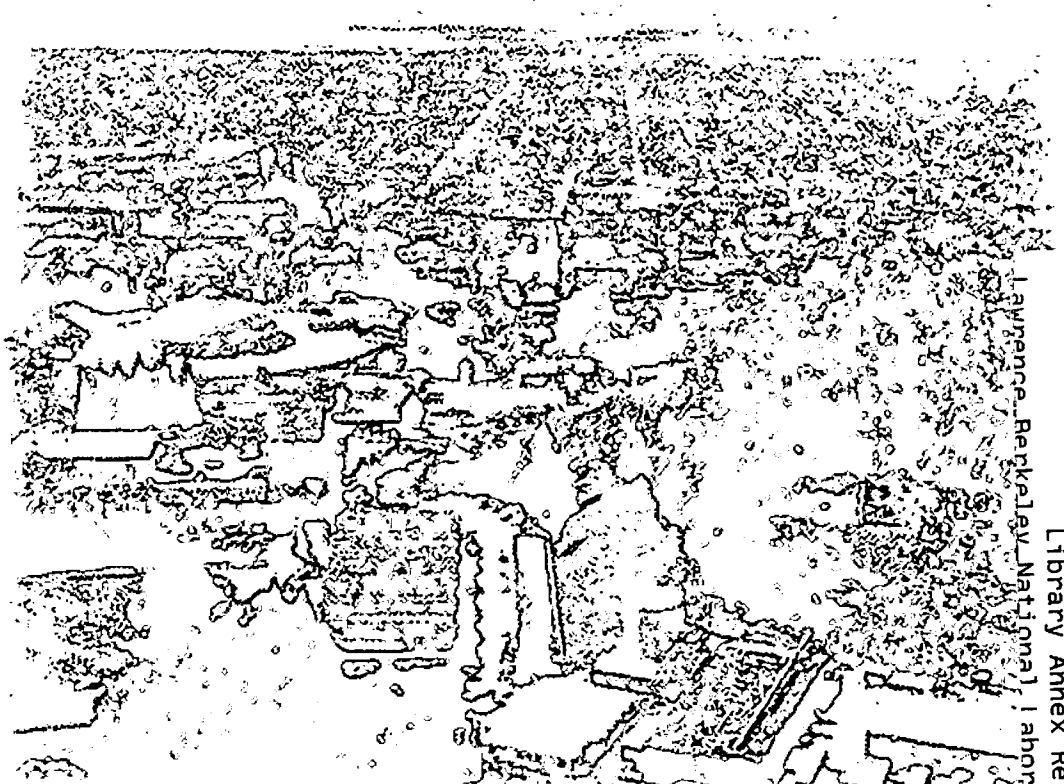

DISCLAIMER

LBNL-46695

POTENTIAL IMPACTS OF CLIMATE CHANGE ON TROPOSPHERIC OZONE IN CALIFORNIA:

A PRELIMINARY EPISODIC MODELING ASSESSMENT OF THE LOS ANGELES BASIN AND THE SACRAMENTO VALLEY

Haider Taha
Staff Scientist, Heat Island Group
Lawrence Berkeley National Laboratory
Berkeley, California

January 2001

This effort was supported by the Union of Concerned Scientists, Roland Hwang, Project Manager, under Award BG-0025500 and by the Assistant Secretary for Energy Efficiency and Renewable Energy, Building Technologies, of the U.S. Department of Energy under contract DE-AC03-76SF00098.

Table of Contents

List of Tables and Figures
Acknowledgements v
1. Summary 1
2. Background 2
3. Assumptions 3
4. Method, data and models 5
    4.1 GCM data 6
    4.2 Air quality models 7
    4.3 Base-case modeling episodes, domains, and emissions 7
    4.4 Climate-change scenarios 8
5. Results 8
    5.1 Controlled vs. non-controlled emissions 9
    5.2 Base-case conditions 9
        5.2.1 Los Angeles Basin 9
        5.2.2 Sacramento Valley 10
    5.3 Future-year/climate change scenarios 10
        5.3.1 Los Angeles Basin 10
            Changes in peak and largest changes 11
            Domain-wide effects 11
            Ozone-temperature correlations 13
        5.3.2 Sacramento Valley 15
            Changes in peak and largest changes 15
            Domain-wide effects 16
            Ozone-temperature correlations 17
        5.3.3 Impacts of non-controlled emissions 18
            Los Angeles Basin 18
            Sacramento Valley 19
    5.4 Significance of predicted air quality impacts 21
6. Model performance evaluation 22
7. Issues, concerns, and research needs 22
8. Conclusions 23
9. References 25

List of Tables

Table 1	Temperature summaries selected from GCM output	6
Table 2	Baseline emission scenarios	8
Table 3	Changes in ozone in the Los Angeles Basin	11
Table 4	Concentrations above thresholds (Los Angeles Basin)	12
Table 5	Domain-averaged concentrations, Los Angeles Basin	13
Table 6	Ozone-temperature correlations (slopes), Los Angeles Basin	14
Table 7	Changes in ozone in the Sacramento Valley	16
Table 8	Concentrations above thresholds (Sacramento Valley)	16
Table 9	Domain-averaged concentrations, Sacramento Valley	17
Table 10	Ozone-temperature correlations (slopes), Sacramento Valley	17
Table 11	Impacts of non-controlled emissions – Los Angeles Basin	19
Table 12	Impacts of non-controlled emissions – Sacramento Valley	19
Table 13	Impacts of controlled vs. non-controlled emissions	20

List of Figures

Figure 1	Simulated base-case peak ozone concentrations, LA Basin	27
Figure 2	Ozone differences at time of peak, LA Basin, CCMA 2010	28
Figure 3	Ozone differences at time of peak, LA Basin, CCMA 2050	28
Figure 4	Ozone differences at time of peak, LA Basin, CCMA 2090	28
Figure 5	Ozone differences at time of peak, LA Basin, HCM 2010	28
Figure 6	Ozone differences at time of peak, LA Basin, HCM 2050	29
Figure 7	Ozone differences at time of peak, LA Basin, HCM 2090	29
Figure 8	Simulated base-case peak ozone concentrations, SV	30
Figure 9	Ozone differences at time of peak, SV, CCMA 2010	31
Figure 10	Ozone differences at time of peak, SV, CCMA 2050	31
Figure 11	Ozone differences at time of peak, SV, CCMA 2090	31
Figure 12	Ozone differences at time of peak, SV, HCM 2010	31
Figure 13	Ozone differences at time of peak, SV, HCM 2050	32
Figure 14	Ozone differences at time of peak, SV, HCM 2090	32

ACKNOWLEDGEMENTS

This effort was supported by the Union of Concerned Scientists, Roland Hwang, Project Manager, under Award BG-0025500 and by the Assistant Secretary for Energy Efficiency and Renewable Energy, Building Technologies, of the U.S. Department of Energy under contract DE-AC03-76SF00098. Jason Mark and Julia Levin, of the Union of Concerned Scientists, are acknowledged for their support and guidance.

The author acknowledges assistance in obtaining UAM input data from the California Air Resources Board (special thanks to E. Mulberg) and the South Coast Air Quality Management District (special thanks to S. Mitsutomi). The author also acknowledges information from GCM models output, special thanks to C. Tonne and Janine Bloomfield of Environmental Defense and R. Goldberg of GISS.

The Heat Island Group at the Lawrence Berkeley National Laboratory is acknowledged for providing the research environment and tools, and computing facilities. Systems Applications International (SAI) and Environ, Inc. are acknowledged for making available different versions of the Urban Airshed Model. MCNC is acknowledged for use of PAVE, a visualization tool for analysis of UAM input and output.

1. SUMMARY

In this preliminary and relatively short modeling effort, an initial assessment is made for the potential air quality implications of climate change in California. The focus is mainly on the effects of changes in temperature and related meteorological and emission factors on ozone formation. Photochemical modeling is performed for two areas in the State: the Los Angeles Basin and the Sacramento Valley.

This study is meant to complement other, ongoing long-term research in this field by providing assessments that may be more consistent with the California air districts' own attainment demonstration modeling procedures and emissions/meteorology data. For this purpose, two versions of the Urban Airshed Model (UAM) were used in this study. The UAM-IV-6.22 was used in simulating the Los Angeles Basin and UAM-IV-5.52 was used for the Sacramento Valley. In both cases, most of the simulation was done using emission inventories with committed future-year controls. This was done to obtain a more realistic and conservative assessment of possible impacts of climate change as stricter emission controls are gradually implemented and the regions approach attainment status with respect to ozone. In addition, emission inventories representing relatively smaller levels of control were also used in limited simulations in this study. The simulated impacts of climate change (e.g., effects of higher temperatures) would be much larger if *current* levels of precursor emissions were used instead of future emissions.

The episodic simulations performed in this study suggest significant implications from potential climate change in California. In the Los Angeles Basin, increases in ozone as large as 26 ppb (~24%) could occur and in the Sacramento Valley, up to 12 ppb (~10%). Such large increases occur near but not at the exact locations of the peaks. At the locations *and* times of the domain base-case peaks, the increases in ozone are relatively smaller but still significant. In the Los Angeles Basin, the domain peak increases by up to 4 ppb and in the Sacramento Valley by up to 9 ppb. The peak concentrations anywhere in the domain can increase by 11 ppb in the Los Angeles Basin and by up to 9 ppb in the Sacramento Valley. The climate change scenarios examined in this study would bring the Los Angeles Basin and the Sacramento Valley out of compliance and increase the severity of the ozone problem. The total area-weighted times (hours) with exceedance concentrations more than double in the Los Angeles Basin and the Sacramento Valley. Using non-controlled emissions, ozone increases as large as 31 ppb can occur in the Los Angeles Basin and the peak (at location and time of base-case peak) increases by up to 12 ppb. Peak concentrations anywhere in the domain (new peaks) increase by up to 25 ppb. In the Sacramento Valley, the non-controlled emissions result in largest increases of up to 15 ppb anywhere in the domain and the peak (at location and time of base-case peak) increases by up to 10 ppb.

The relative impacts on air quality reported in this study might be of greater interest than the absolute impacts. For instance, attainment assumptions for the Los Angeles Basin are different than those for the Sacramento Valley, and these are reflected in the correspond-

ing emission inventories. Thus results for these two regions cannot be directly compared. Finally, the results presented in this report are episode- and region-specific and, thus, may not provide a suitable basis for generalization to other time periods or regions, or to develop indications for historical trends in ozone air quality. The results suggest that the ozone air quality impacts of climate change should be further investigated, modeled, and analyzed in the future in a more detailed, full-blown modeling approach.

2. BACKGROUND

Climate change and its potential environmental implications are issues of growing concern. One aspect of interest is the possible role climate change could play in worsening the air quality, e.g., impacts on tropospheric ozone formation. This study is a preliminary effort aiming to quantify the potential implications of climate change on ozone air quality in two California regions, in a fashion that may be more compatible with the local air districts' modeling methodologies and consistent with their emissions and meteorology data.

The premise of this and similar studies is that ozone air quality is profoundly affected by changes in climate and meteorology. Temperature, winds, solar radiation, atmospheric moisture, venting and mixing, affect both the photochemical production of smog as well as the emissions of ozone precursors (e.g., NOx and VOC) that are temperature- and solar-radiation dependent. For example, biogenic hydrocarbon emissions are particularly sensitive to changes in air temperature and solar radiation. In addition, meteorology affects the transport, dispersion, and deposition of pollutants and precursors alike.

There has been some focus on the potential impacts of changes (e.g., increases) in air temperature on ozone air quality. Air temperature has a direct effect on photochemical reactions producing ozone, e.g., chemistry of PAN (Sillman et al. 1990) as well as emissions of precursors. But temperature is also an indirect indicator to other mechanisms that can accelerate smog formation. These include, stalled high-pressure systems, intensified subsidence, reduced cloud cover, increased atmospheric water vapor, etc. Thus in this sense, temperature is a surrogate for many other exacerbating factors.

In this study, the focus is on the effects of changes in temperature, mixing, and emissions of biogenic hydrocarbons on the formation of troposheric ozone. Modeling studies of this nature have been performed in the past, e.g., Sillman and Samson (1995), and focused on roughly similar parameters, e.g., temperature and PAN reaction rates, biogenic emissions, and photolysis rates. However, that study did not account for the effects of changing vertical mixing, and was done at a relatively coarser resolution than the present study. In both studies, wind speeds were unchanged.

This modeling work is an extension of previous effort in analyzing the role of meteorology in air quality, e.g., Taha (1996,1997), Taha and Bornstein (1999), and Taha et al.

(2000,1997). Its purpose is to develop an estimate of the possible impacts of climate change on ozone air quality in California and suggest further modeling, analysis, and research.

3. ASSUMPTIONS

In the GCM simulations that served as a basis for the present air quality modeling work, it was assumed that the baseline climate conditions correspond to the period 1961 through 1990. It was also assumed that CO_2 concentrations increase by 1% per year starting in 1990. Stratospheric ozone is assumed unchanged in this study and, therefore, the UV flux reaching the troposphere is also unchanged.

It is also assumed here that there will be no future changes in inter-basin, inter-state, or inter-continental transport of pollutants through and into the domains of interest. While this assumption may be tolerated for this immediate modeling task, it obviously needs re-evaluation in the future, especially in light of long-range pollutant transport through California, including from overseas.

In this work, only changes in temperature, boundary-layer height, and biogenic hydrocarbon emissions are accounted for. The effects arising from possible changes in the wind field, persistence of subsidence or persistence of the Pacific high-pressure system, atmospheric water vapor, and increased cloudiness, are not accounted for. Meteorology-induced changes in *anthropogenic* precursor emissions are assumed to be relatively small, since absolute emissions will be much smaller in future years as a result of stricter emission controls.

Some of the above assumptions may be justified to a certain extent. For example, solar radiation does not vary significantly (less than 5%), according to the GCM simulations the months and decades considered in this report. In addition, the modeled episodes are cloud-free.

Temperature.
With respect to global-change temperature scenarios, it is assumed here that the space-averaged, time-dependent temperature perturbation, $\overline{T}_t$, (over a domain of interest, e.g., Los Angeles Basin or the Sacramento Valley) can be decomposed as

$$\overline{T}_t = \overline{T}_{tL} + \overline{T}_{tS} + \overline{T}_{tD} \qquad (1)$$

where the subscripts L, S, and D stand for Long-term, Seasonal, and Diurnal perturbations, respectively. Over a domain of interest, the assumption is also made that

$$T_{i,j,k,t} = \overline{T}_t + T'_{i,j,k,t} \qquad (2)$$

and that $T'_{i,j,k,t}$ (spatial deviation) will be no different in the future-year scenarios than they currently are. This assumption is made due to lack of mesoscale detail (lack of mesoscale downscaling of GCM output). Here, i,j,k is the three-dimensional cartesian notation and t is time. A related assumption is that the urban heat island (intensity and extent) is not "grown" for future-year scenarios.

In addition, since the output from GCMs obtained for this modeling effort provided only an indication for the changes in maximum and minimum monthly air temperatures, some interpolation was necessary to develop hourly temperature change profiles for use in photochemical simulations. For the two summer episodes modeled in this study (July in the Sacramento Valley and August in the Los Angeles Basin), the minimum air temperature is reached at around 0500 PDT and the maximum around 1500 PDT. With the temperature changes given at the times of the maxima and minima (from the two GCMs considered in this study) the hourly temperature profile is computed from:

$$\Delta(t) = \mu + \frac{1}{2}\Delta.F(t) \qquad (3)$$

where $\Delta(t)$ is the time-dependent temperature (e.g., hourly) difference between a GCM scenario and today's conditions, μ is the mean of the predicted change in temperature (mid-range of GCM-predicted temperature changes at times of maxima and minima), Δ is the total range of predicted change in temperature, and the scaling factor F(t) is given by:

$$F(t) = a\cos(\frac{2\pi t}{24}) + b\sin(\frac{2\pi t}{24}) \qquad (4)$$

where, in this case, a = 0.531 and b = 0.889.

Mixing height.
Changes in the mixing height are approximated based on previous modeling sensitivity analysis for the Los Angeles Basin and the Sacramento Valley, as applicable to each region (Taha et al. 2000, Taha et al. 1997). These approximations were based on computation of changes in turbulent kinetic energy (TKE) as a function of temperature change near the ground or on relatively simpler approximations, such as those proposed by Benkley and Schulman (1979).

In this study, the changes in mixing height are mapped onto the original mixing height field input to the UAM. Sensitivity simulations suggest that if the increase in mixing height is not accounted for, the effect of temperature rise on ozone air quality can be larger than reported here, due to relatively smaller venting and dilution rates (Taha et al. (1997).

Biogenic hydrocarbon emissions.
In this study, only emissions of isoprene are modified to reflect the impacts of future-year temperature (and solar radiation) changes. Isoprene emissions generally account for more than 80% of total biogenic hydrocarbon emissions. In addition, the changes in this study account mainly for temperature differences since there is no significant change in solar radiation predicted by the GCMs for the months and decades selected in this report. Also, the modeled episodes are assumed to be cloud-free.

The adjustments of isoprene emissions were done based on an environmental correction algorithm (Guenther et al. 1993) and then mapped on the original emissions input to the UAM. Use of this algorithm in updating the emissions of isoprene input to UAM is discussed in Taha et al. (2000).

An interesting aspect of this correction is that emissions of isoprene increase up to about 310K and start decreasing afterwards because of increased stomata control beyond that temperature threshold. This is relevant to this study since the predicted future-year daytime temperatures often exceed 310K (particularly for years after 2050) and can actually cause a decline in biogenic hydrocarbon emissions in some cases. This has an impact on the ozone air quality, as will be discussed later in this report.

4. METHOD, DATA, and MODELS

The method employed in this modeling exercise simply involves modifying the meteorological and emissions input to air quality models according to General Circulation Models (GCM) predicted future-year states. Output from two GCMs was obtained. The models are: 1) the United Kingdom Meteorological Office's Hadley Cell Model (hereafter referred to as HCM) and 2) the Canadian Center for Modeling and Analysis model (hereafter referred to as CCMA). As mentioned earlier, the results provided in this report are not meant to replace those from other, ongoing long-term data analysis and research in this field. Rather, the intent is to complement them by providing the California air districts with results that may be relatively more compatible with their own attainment demonstration modeling strategies, e.g., episodic simulations with the Urban Airshed Model (UAM), and relatively more consistent with their emissions and meteorology data.

The GCM output was used to modify original input to UAM via 4-dimensional mapping (Taha et al. 2000) of perturbations in meteorological and emission parameters of interest. This approach was followed so as to produce simulated base-case conditions that are close to an exact replication of the air districts' own simulation results (except for slight variations resulting from small differences in models and related mechanisms). Although this method could sacrifice some accuracy and can potentially introduce errors, it provides an alternative to regenerating all input data, which was not feasible in this short modeling study. In addition, it is often difficult to replicate the districts' modeling results and simulation attributes when using other than their own input data.

4.1 GCM DATA

Table 1 summarizes a selected subset of the GCM temperature scenarios that were obtained for this study. In this table, CCMA and HCM indicate the Canadian and Hadley Cell models, as discussed earlier, GHG indicates green-house-gas increase scenarios, GHG+S indicates scenarios in which both green-house gases and sulfates have increased, and μ and Δ are as defined in equation (3). Scenarios simulated and discussed in this report are those with "GHG+S" from both models.

Table 1. Temperature summaries selected from GCM output for years 2010, 2050, and 2090 (μ and Δ are defined in equation 3).

Scenario ↓		2010	2050	2090
CCMA: GHG		(K)	(K)	(K)
July	μ=	1.28	2.68	7.98
	Δ=	0.22	1.00	1.84
August	μ=	0.44	2.89	5.77
	Δ=	0.13	.46	1.1
CCMA: GHG+S				
July	μ=	3.06	4.03	5.94
	Δ=	0.82	0.81	1.11
August	μ=	0.94	2.36	6.35
	Δ=	1.01	0.05	1.68
HCM: GHG				
July	μ=	1.78	3.05	4.09
	Δ=	0.21	0.66	1.39
August	μ=	1.30	3.07	4.45
	Δ=	0.23	1.02	2.29
HCM: GHG+S				
July	μ=	1.52	1.74	3.52
	Δ=	0.00	0.31	1.13
August	μ=	1.02	1.64	4.08
	Δ=	0.29	0.59	0.90

4.2 AIR QUALITY MODELS

Two versions of the Urban Airshed Model were used in this study. For the Los Angeles Basin, UAM-IV-6.22 was used, whereas for simulating the Sacramento Valley, a more advanced version (UAM-IV-5.52) was employed. Version 6.22 is the "regulatory" UAM approved by the USEPA for demonstration modeling. Different versions were used in this study to accommodate the different input provided by the SCAQMD and the CARB.

The main difference between versions 5.52 and 6.22 is that the former can use 3-dimensional, time-dependent fields of temperature, humidity, and winds as input (e.g., from a meteorological model). Other differences exist in some aspects of the Carbon-Bond IV mechanism, e.g., chemical reaction rates constants. See Taha et al. (2000) for some discussion on this issue. Because of these and other differences, the results from simulating the two regions are not directly intercomparable.

4.3 BASE-CASE MODELING EPISODES, DOMAINS, and EMISSIONS

Two frequently used attainment-demonstration modeling episodes and domains were selected for this study. The modeling domains are shown in the figures at the end of this report. For the Los Angeles Basin, the 2010 projection of the August 26-28, "1987" episode was used. The 2005 projection of the July 11-13, "1990" episode was used for the Sacramento Valley. The reason for selecting future-year projections of the inventories is the assumption that future-year climate change will occur at a time when some or all committed emission controls are in place. Although the climate change scenarios in this study span all the way to year 2090, the emissions inventories, in theory, do not go beyond about 2020.

All emissions, controlled scenarios, domains, and episodes are described in SCAQMD (1996) and CARB (1995), and will not be repeated here. In this study, two baseline emission scenarios for each region were simulated. One baseline scenario represents a "controlled" case, whereas the other represents a scenario with relatively less stringent controls. These are summarized in **Table 2**, and will be referred to in this report as "controlled" and "non-controlled" emissions. Note that the numbers in **Table 2** are taken directly from the UAM itself, as used in this study, and may or may not be directly comparable to numbers reported by the air districts in their air quality plans and related publications. **Table 2** lists emissions in mtpd (metric tons per day) for the last day of the modeling episode for each region. These emission levels are for present-day climate and are further modified in this study for future-year (climate change) scenarios.The last column gives emission totals for VOC and biogenic VOC.

Table 2. Baseline emission scenarios as simulated in this study. Units are mtpd on last day of episode.

Region	*Scenario*	*NOx*	*VOC+BVOC*
Los Angeles Basin	Non-controlled base case	641	771
	Controlled base case	578	610
Sacramento Valley	Non-controlled base case	214	893
	Controlled base case	153	766

4.4 CLIMATE-CHANGE SCENARIOS

In this short project, only the following scenarios were simulated and analyzed: 1) only cases GHG+S (green house gases plus sulfates) from both models were simulated, 2) only three decades (2010, 2050, 2090) were considered, 3) only controlled future-year emissions were used (along with a smaller set of simulations using non-controlled emissions, as shown in Table 2), and 4) all meteorological/emissions changes were lumped into one scenario for each region. The difference between cases GHG and cases GHG+S can be seen (in terms of temperature) in **Table 1**. Generally, the inclusion of increased sulfates in the GCM simulations can cause a relative increase in albedo over the oceans (Trenberth 1992) leading to some differences (e.g., relative cooling over the oceans) with respect to cases with GHG-only increase.

5. RESULTS

In this section, results from the last day of each region's episode are presented. Furthermore, only results for the lowest layer of the atmosphere (first layer of the UAM) are discussed. In some cases, the results are specific to certain hours, e.g., peak time, as defined in the discussion.

In going through the rest of this report, one would be tempted to compare the results from the Los Angeles simulations to those from the Sacramento Valley's. Thus it is appropriate to point out again that the modeling results for these two regions are not directly intercomparable. This is due to several reasons, the main ones being that 1) different models were used in simulating these regions, 2) different attainment and emission inventory assumptions were made, and 3) the GCM forecast for these two regions is different.

5.1 Controlled vs. non-controlled emissions

The bulk of this modeling work was done using future-year controlled emissions. The emission inventories and their variants are explained in CARB (1995) and SCAQMD (1996). In addition, limited simulations were also performed with emissions that have relatively smaller level of control. In this report, these scenarios will be termed "controlled" and "non-controlled". This may not be exactly what the air districts define, but is a relative term in this context.

In terms of base-case air quality conditions, the effects of using these different emission baselines were found to be significant. For example, the peak ozone in the Los Angeles basin decreases from the neighborhood of 118 ppb, with non-controlled, down to 110 ppb with controlled emissions. For the Sacramento Valley, the domain peak decreases from 139 ppb down to about 120 ppb.

For clarity, the following sections will present results of simulations with controlled emission baselines only. The effects of climate change simulated with non-controlled baseline emissions will be discussed separately in Section 5.3.3.

5.2 Base-case conditions

This section briefly describes the simulated base-case conditions for **current** climate with controlled emissions. These emission baselines correspond to those of year 2010 (under current climate conditions) for the Los Angeles Basin and year 2005 (under current climate conditions) for the Sacramento Valley.

5.2.1 Los Angeles Basin

The SCAQMD has assumed a significant level of emission control in place by the year 2010. This assumption is reflected in the controlled emissions baseline (used in this study) and, as a result, no violations of the standard are seen in the base-case conditions. The simulated base-case peak on the last day of the modeling episode (August 28) occurs at 1500 PDT. The simulations show that during the peak hour, concentrations are highest in north San Fernando Valley, north Ontario, in Riverside, and the San Jacinto Valley (south east of Riverside), as seen in **Figure 1**. The peak is about 110 ppb occurring in the San Jacinto Valley region. With respect to the current California standard of 90 ppb, there are many non-compliant regions in this base-case scenario, even with controlled emissions (as will be seen in **Table 4**).

5.2.2 Sacramento Valley

The simulated base-case peak concentration on the last day of the modeling episode for Sacramento (July 13) occurs at 1700 PDT (**Figure 8**). The highest concentrations are found along the Sacramento-Auburn "corridor" and the peak amounts to 120 ppb in an area just northeast of Sacramento. With respect to the current California threshold of 90 ppb, there are many regions out of compliance in this base-case scenario, even with controlled emissions (as will be seen in **Table 8**).

5.3 Future-year/climate change scenarios

In this section, the simulated impacts of selected climate-change scenarios are discussed. These account mainly for the effects of temperature change predicted by GCMs, in addition to related meteorological and emission modifications, as explained in Sections 3 and 4. As noted earlier, it is perhaps more interesting to track the relative air quality implications (ozone changes) than the absolute ones, because the latter depend relatively more on the attainment assumptions and the corresponding emission data.

5.3.1 Los Angeles Basin

Changes in peak and largest changes

Compared to the base-case peak of 110 ppb at 1500 PDT, the peak in case CCMA GHG+S YEAR 2010 is 111 ppb, occurring at the same location as that of the base-case scenario (grid 42,14). While this represents an increase of only 1 ppb in the peak, there are increases of up to 3 ppb in other areas of the domain (**Figure 2**). For case CCMA GHG+S YEAR 2050, the peak is 113 ppb still at the same location (an increase of 3 ppb). However, there are now increases as large as 11 ppb elsewhere (as seen in **Figure 3**) and the increased concentrations affect a larger area. For case CCMA GHG+S YEAR 2090, the peak occurs at 1400 instead of 1500 PDT and amounts to 121 ppb (an increase of 11 ppb with respect to the base-case peak). The location also changes, so that the peak is now at grid 34,19. However, at the time of the base-case peak (1500 PDT), the new peak in 2090 under this scenario is 120 ppb but again, at grid 34,19.

Thus in this scenario, the Los Angeles Basin is in non-compliance with respect to the 120 ppb NAAQS. As seen in **Figure 4**, there are increases of up to 26 ppb in the domain, leading to the new peak and higher concentrations in surrounding areas. In this scenario, there can also be small decreases of 1 or 2 ppb in some very limited areas in the domain because of decreased BVOC emissions (as temperature exceeds 310K) and also because of the increase in mixing height.

For case HCM GHG+S YEAR 2010, the peak occurs at 1500 PDT and at the same location as that of the base-case. The new peak is about 111 ppb, only 1 ppb

higher than in the base case. However, there are, in this scenario, increases of up to 4 ppb, as seen in **Figure 5**. In case HCM GHG+S YEAR 2050, the peak is 112 ppb at the same time and location of the base-case's, and there are increases of up to 7 ppb elsewhere in the domain (**Figure 6**). Finally, in scenario HCM GHG+S YEAR 2090, the peak is 114 ppb occurring at 1400 instead of 1500 PDT and at grid 34,19 instead of 42,14. At 1500 PDT (time of base-case peak), the new peak corresponding to HCM GHG+S YEAR 2090 is 113 ppb and occurs at the location of the base-case peak. Although the changes in the peaks are relatively small, elsewhere in the domain there are increases of up to 17 ppb (which is causing the new peak at 1400) and a decrease of up to 1 ppb, as seen in **Figure 7**. The reason for the small decreases in concentrations was explained earlier. **Table 3** summarizes these results.

Table 3. Changes, peaks, and largest changes in the Los Angeles Basin. (Entries are in ppb [O3] and %)

	P(TL)	Δ	Δ%	P(any)	Δ	Δ%	ΔL	Δ%
CCMA: GHG+S 2010	111	1	0.9	111	1	0.9	3	2.7
CCMA: GHG+S 2050	113	3	2.7	113	3	2.7	11	10
CCMA: GHG+S 2090	114	4	3.6	121	11	10	26	23.6
HCM: GHG+S 2010	111	1	0.9	111	1	0.9	4	3.6
HCM: GHG+S 2050	112	2	1.8	112	2	1.8	7	6.3
HCM: GHG+S 2090	113	3	2.7	114	4	3.6	17	15.4

P(TL)=Peak at time and location of base-case peak; P(any)=Peak anytime anywhere in domain (during the last day of episode); Δ= Difference from base-case peak; ΔL=Largest increase anytime during the last day of the episode and anywhere in domain (unrelated to other columns); Δ%= Percent change with respect to base-case domain peak.

Table 3 shows that one entry is in violation with respect to the NAAQS of 120 ppb, but with respect to the CAAQS of 90 ppb or the proposed 8-hour standard of 80 ppb, all entries show non-compliance.

Domain-wide effects:

For this analysis, the entire last day of the modeling episode is considered first, then the hour at the base-case peak (1500 PDT) on that day is examined. All grids in the domain minus two grid rows at the boundaries (to discard boundary effect) were considered and the results are shown in **Table 4**. Note that absolute (not relative) values are given in this table, since relative values, e.g., percent area, depend on the definition of the averaging domain, which, for this purpose, can be quite arbitrary.

Table 4. Space-time aspects of concentrations above thresholds (Los Angeles Basin) during last day of episode.

Case	Km^2.hr [O3]≥120 ppb	Km^2.hr [O3]≥90 ppb
Base-case	0	4612
CCMA: GHG+S 2010	0	5139 (Δ=11%)
CCMA: GHG+S 2050	0	6720 (Δ=46%)
CCMA: GHG+S 2090	50	9750 (Δ=110%)
HCM: GHG+S 2010	0	5402 (Δ=17%)
HCM: GHG+S 2050	0	5929 (Δ=29%)
HCM: GHG+S 2090	0	8037 (Δ=74%)

The second and last columns in this table give the value of "area × time" when the concentrations are higher than the specified threshold. Thus, if a grid cell in the domain has concentrations over the threshold (120 or 90 ppb) for one hour, it will register as 1 grid.hr above the respective threshold, which is then converted to km^2.hr by multiplying by the grid-cell area (25 km^2 for the Los Angeles Basin modeling domain). The percentage change in the last column is with respect to the base-case entry (top entry in the last column), and shows that the relative impact can be very significant, e.g., more than doubling the area and times affected by exceedance concentrations. The middle column does not show percentages since a percentage with respect to zero is meaningless.

In **Table 5**, domain-averaged concentrations (all grids within the domain minus two rows near the boundaries) of ozone during the last 24 hours of the episode and during the time of the base-case peak are given. Thus increases in the domain-averaged ozone concentrations can reach up to 3.6% on a diurnal basis and up to 2.9% at the time of the base-case peak. Considering the large number of grids in the domain, the changes are significant. A visual examination of **Figures 3 through 7** reveals that the area affected by the increased ozone is quite large, covering almost the entire South Coast Air Basin. Thus even though the increase in concentrations may be relatively small, the large aerial extent of the changes makes the impacts significant.

Table 5. Domain-averaged concentrations, Los Angeles Basin

Case	24-hr Domain-averaged [O3]	Peak-hour domain-averaged [O3]
Base-case	46.9 ppb	58.0 ppb
CCMA: GHG+S 2010	47.2 ppb (Δ=0.6%)	58.2 ppb (Δ=0.3%)
CCMA: GHG+S 2050	47.7 ppb (Δ=1.7%)	58.8 ppb (Δ=1.4%)
CCMA: GHG+S 2090	48.6 ppb (Δ=3.6%)	59.7 ppb (Δ=2.9%)
HCM: GHG+S 2010	47.3 ppb (Δ=0.8%)	58.4 ppb (Δ=0.7%)
HCM: GHG+S 2050	47.4 ppb (Δ=1.1%)	58.5 ppb (Δ=0.8%)
HCM: GHG+S 2090	48.1 ppb (Δ=2.5%)	59.3 ppb (Δ=2.2%)

Ozone-Temperature correlations:

Since temperature is one of the most interesting aspects of climate change and weather in general, there has been some historical interest in correlating ozone changes to those in temperature. This is often done despite the fact that temperature is *only one* of many independent variables that can contribute to ozone concentration changes. In this section, an indication to this correlation is given, subject to caveats, such as:

1. Correlating to temperature provides only partial insight into the smog-formation process and its dependence on meteorology. Other factors, such as winds, water vapor, mixing, transport, emissions, etc., should also be accounted for.
2. Since only some aspects of simulated maximum ozone and temperature are examined in this exercise, the statistical sample is extremely small (7 to 10 points) in these episodic simulations.
3. The range of temperature considered in this correlation is narrow (~5K), thus the applicability of the correlation may be limited to this given range.
4. The absolute maximum temperatures examined in this section are generally larger than 308 or 314K (see table below). Above such temperature thresholds, there is 1) typically a large observed scatter in ozone concentrations resulting in a weak correlation, 2) a decrease in biogenic hydrocarbon emissions (which can affect the ozone formation rate), and 3) not much measured data is available to compare with (e.g., data such as from EPA 1996).

Thus the validity of the correlations developed here should be carefully kept in perspective by acknowledging these limitations. **Table 6** summarizes the correlations along with some statistical indicators. One needs to keep in mind the caveats mentioned above and also that the correlations are valid only within the temperature range given in the third column. Here, R^2 is the correlation coefficient and S

is the T-test statistics. All entries in this table (except last row) correspond to controlled emission inventories.

Table 6. Ozone-temperature correlations based on simulated climate-change scenarios.

	ppb/K	Range (K)	R^2	S
Peak ozone at time and location of base-case peak	0.67 (1)	308<T<315	0.88	0.0018
Peak ozone anytime anywhere in domain	1.80 (2)	314<T<321	0.91	0.0009
Largest ozone increase anytime anywhere in domain	4.61 (3)	314<T<321	0.99	0.0001
Largest ozone increase anytime anywhere in domain	15.0 ‡			

‡ *This slope corresponds to non-controlled emission inventories as used in the historical 1987 modeling episode of the Los Angeles Basin (Taha et al. 1994,1997). The meteorological changes, however, were confined mainly to urbanized areas and surrounds. In these studies, the sensitivity of ozone concentrations to changes in temperature was found to be in the range of up 15 ppb/K (last row in the table), but about 8-10 ppb/K in general.*

Table notes:

(1) Temperature used in developing this correlation is that at the same time and location as the base-case peak.

(2) Temperature used in developing this correlation is the maximum anywhere in the domain but at the same time as the peak in this case (the new domain peak).

(3) Temperature used in developing this correlation is maximum temperature anywhere in the domain but at same time as largest increase in ozone.

There are several reasons why the slopes in **Table 6** are 1) smaller than the one in the last row and 2) why these slopes may not be directly comparable to those reported elsewhere, for example, by EPA (1996,1988). Some of these reasons are:

1) The larger slopes reported elsewhere in the literature were based on present-day levels of precursor emissions, whereas the simulations here are based on future-year controlled-emission scenarios. Thus the effects of meteorology (temperature) on emissions and chemical reactions are relatively smaller.
2) The range of absolute temperatures simulated here is higher than that used in developing correlations reported elsewhere (also, the simulations are for warmer future-year weather for which there are no corresponding historical observations). Thus there is no basis for direct comparison. In addition, the correlation weakens above 308K (when mixing intensifies and the boundary layer rises significantly), and the slope (with respect to temperature) becomes generally smaller.

3) The range of air temperature over which the present correlations are developed (~5K) is smaller than the range used in previous studies (~ 30K) and this may contribute to weaker correlations or smaller slopes in this study.
4) Unlike the long-term correlations reported in other research, the results in this report are episodic, i.e., they are neither transferable to nor comparable with those from other times, meteorological conditions, or regions.
5) The reference temperature used in developing such correlations can play a significant factor in the strength (slope) of these relations. In the Los Angeles Basin, for example, temperature varies significantly from the ocean towards the inland areas and enclosed valleys, making it difficult to select a representative reference point for use in developing these correlations. For example, some researchers have developed ozone-temperature correlations using temperature data from LAX, which is on the ocean side where temperature fluctuation is dampened and absolute temperature is usually lower than inland. Thus using maximum ozone (which happens inland) vs. ocean-side temperature can result in correlations that are different from those reported here.

5.3.2 Sacramento Valley

Changes in peak and largest changes

As mentioned earlier, the simulated base-case peak in the Sacramento Valley amounts to 120 ppb and occurs at 1700 PDT, northeast of Sacramento. In case CCMA GHG+S YEAR 2010, the new peak is 128 ppb occurring at the same location as in the base-case scenario (grid 31,22). This increase of 8 ppb over the base-case concentrations (**Figure 9**) is also the largest anywhere in the domain. For case CCMA GHG+S YEAR 2050, the peak is again 128 ppb and still occurs at the same location. However, there are now increases as large as 10 ppb elsewhere (**Figure 10**). The largest increases occur in the Sacramento-Auburn corridor, especially northeast of Sacramento. For case CCMA GHG+S YEAR 2090, the peak amounts to 129 ppb and occurs at the same location as the base-case peak. But as seen in **Figure 11**, there are now increases of up to 12 ppb in the northeast portion of the domain. There can also be decreases of 1 or 2 ppb in very limited areas as a result of decreased BVOC emissions (as temperature exceeds 310K) and also in part because of the increase in mixing.

For case HCM GHG+S YEAR 2010, the peak is 127 ppb occurring at the same time and location as that of the base-case. The increase of 7 ppb (**Figure 12**) is also the largest anywhere in the domain. In case HCM GHG+S YEAR 2050, the changes are similar to those in case HCM GHG+S YEAR 2010, except for some differences in the spatial distribution of these changes (**Figure 13**). Finally, in scenario HCM GHG+S YEAR 2090, the peak is 128 ppb, but elsewhere in the domain, there are increases of up to 9 ppb as seen in **Figure 14. Table 7** gives summaries for these and other results. The Sacramento Valley is in non-compliance regardless of the scenario being analyzed.

Table 7. Changes, peaks, and largest changes in the Sacramento Valley. (Entries are in ppb [O3] and %)

	P(TL)	Δ	Δ%	P(any)	Δ	Δ%	ΔL	Δ%
CCMA: GHG+S 2010	128	8	6.7	128	8	6.7	8	6.7
CCMA: GHG+S 2050	128	8	6.7	128	8	6.7	10	8.3
CCMA: GHG+S 2090	129	9	7.5	129	9	7.5	12	10
HCM: GHG+S 2010	127	7	5.8	127	7	5.8	7	5.8
HCM: GHG+S 2050	127	7	5.8	127	7	5.8	7	5.8
HCM: GHG+S 2090	128	8	6.7	128	8	6.7	9	7.5

P(TL)=Peak at time and location of base-case peak; P(any)=Peak anytime anywhere in domain (during the last day of episode); Δ= Difference from base-case peak; ΔL=Largest increase anytime during the last day of the episode and anywhere in domain (unrelated to other columns); Δ%= Percent change with respect to base-case domain peak.

Domain-wide effects:

For this analysis, the entire last day of the modeling episode was examined first, and then the base-case peak hour (1700 PDT) on that day was analyzed. All grids in the domain minus two grid rows at boundaries (to discard boundary effect) were considered. **Tables 8 and 9** summarize the results.

Table 8. Space-time aspects of concentrations above thresholds (Sacramento Valley) during the last day of the episode.

Case	Km^2.hr [O3]≥120 ppb	Km^2.hr [O3]≥90 ppb
Base-case	0	3483
CCMA: GHG+S 2010	208	5723 (Δ=64%)
CCMA: GHG+S 2050	224	5972 (Δ=71%)
CCMA: GHG+S 2090	240	6221 (Δ=77%)
HCM: GHG+S 2010	192	5433 (Δ=56%)
HCM: GHG+S 2050	192	5433 (Δ=56%)
HCM: GHG+S 2090	224	5806 (Δ=67%)

The middle and last columns in **Table 8** give the value of "area × time" when the concentrations exceed the specified threshold, as explained in section 5.3.1., except that the grid-cell area is 16 km^2 in the Sacramento Valley modeling domain. The percentage change in the last column is with respect to the base-case entry (top entry in the last column), and shows that the relative impact can be very significant, e.g., roughly doubling the area and times of exceedance concentrations.

No percentages are given in the middle column since a percentage with respect to zero is meaningless.

In **Table 9**, domain-averaged concentrations (averaged over all grids within the domain minus two rows near the boundaries) of ozone during the last 24 hours of the episode and at the time of the base-case peak concentrations are given. The results show that increases in the domain-averaged ozone concentrations can reach up to 4.8% on a diurnal basis and up to 4.0% at the time of the base-case peak, which is quite significant, given the large number of grids in the domain. A visual examination of **Figures 9 through 14** reveals that the area affected by increased ozone concentrations is quite large; almost the entire domain.

Table 9. Domain-averaged concentrations, Sacramento Valley

Case	24-hr Domain-averaged [O3]	Peak-hour domain-averaged [O3]
Base-case	39.5	62.3
CCMA: GHG+S 2010	40.9 (Δ=3.5%)	64.5 (Δ=3.5%)
CCMA: GHG+S 2050	41.1 (Δ=4.1%)	64.6 (Δ=3.7%)
CCMA: GHG+S 2090	41.4 (Δ=4.8%)	64.8 (Δ=4.0%)
HCM: GHG+S 2010	40.5 (Δ=2.5%)	64.2 (Δ=3.0%)
HCM: GHG+S 2050	40.6 (Δ=2.8%)	64.2 (Δ=3.0%)
HCM: GHG+S 2090	41.0 (Δ=3.8%)	64.5 (Δ=3.5%)

Ozone-Temperature correlations:

An indication to the ozone-temperature slope is given here for the Sacramento Valley, subject to the caveats mentioned earlier in section 5.3.1. It is very important to keep these restrictions in mind (especially since temperature is *only one* of many variables that need to be accounted for) when examining the results given here. **Table 10** summarizes these correlations (slopes) along with some statistical indicators. One also needs to keep in mind that the correlations are valid mainly within the temperature range given in the third column of the table. Here, R^2 is the correlation coefficient and S is the T-test statistic. All entries in this table (except last row) correspond to controlled emission inventories.

Table 10. Ozone-temperature correlations based on simulated climate-change scenarios (Sacramento Valley).

	ppb/K	Range (K)	R^2	S
Peak ozone at time and location of base-case peak	1.4 (1)	310<T<317	0.63	0.0314
Peak ozone anytime anywhere in domain	1.4 (2)	311<T<317	0.65	0.0294
Largest ozone increase anytime anywhere in domain	2.0 (3)	311<T<317	0.86	0.0027
Largest ozone increase anytime anywhere in domain	8.3 ‡			

‡ *This slope corresponds to the non-controlled emission inventories as used in the 1990 modeling episode for the Sacramento Valley (Taha et al. 2000). The meteorological changes in that study were confined to urban areas and immediate surrounds. In these studies, the sensitivity of ozone concentrations in the Sacramento Valley to changes in temperature was found to be in the range of up to 8.3 ppb/K (last row in the table).*

Table notes:
(1) Temperature used in developing this correlation is that at the same time and location as the base-case peak.
(2) Temperature used in developing this correlation is the maximum anywhere in the domain but at the same time as the peak in this case (the new domain peak).
(3) Temperature used in developing this correlation is maximum temperature anywhere in the domain but at same time as largest increase in ozone.

The correlations are relatively weaker than those obtained for the Los Angeles Basin (discussed in Section 5.3.1) and the slopes are relatively smaller. The correlation can improve significantly (for the Sacramento valley) if the base-case scenario is excluded from the linear regression or, alternatively, if non-linear regression is employed.

As discussed earlier, one should note again that the slopes given in the second column may not be directly comparable to those reported in the literature, for example, by EPA (1996,1988). Refer to Section 5.3.1 for reasons and concerns.

5.3.3 Impacts of non-controlled emissions

In this section, the impacts of climate-change scenarios with non-controlled emissions are presented. Recall that the definition of controlled and non-controlled emissions is relative to this study (as defined in Table 2) and is not a "universal" definition with respect to that used by the air districts.

Los Angeles Basin

For the Los Angeles Basin, the base-case peak corresponding to non-controlled baseline emissions is 118 ppb on August 28 at 1500 in cell 35,18. The simulation of climate-change scenarios suggests that there are increases at the location **and** time of the base-case peak. There are also new peaks elsewhere in the domain and at other times. **Table 11** summarizes these results, for only two CCMA scenarios.

Table 11. Simulated impacts with non-controlled emissions. Los Angeles Basin, last day of episode.

	New peak at location and time of base-case peak (base=118 ppb)	New domain peak any time and location during last day	Largest increase anywhere in the domain
CCMA: GHG+S 2050	123 ppb (Δ = 5 ppb)	127 ppb (Δ = 9 ppb)	Δ = 13 ppb
CCMA: GHG+S 2090	130 ppb (Δ = 12 ppb)	143 ppb (Δ = 25 ppb)	Δ = 31 ppb

Column 2 gives the new peak at *the location and time of the base-case peak*, whereas column 3 shows the new domain peak (at other times and locations). Thus the new domain peak is 127 (at 1400 and cell 34,19) for year 2050 and 143 ppb (at 1500 and cell 34,19) for year 2090, respectively. The new peak is in a cell neighboring the original location of the base-case peak. The last column shows the largest increases in ozone during the last day of the modeling episode (anywhere in the domain and anytime during the last day). Both 13-ppb and 31-ppb increases occur in cell 34,19 and at 1500.

Sacramento Valley

In the Sacramento Valley, the simulations with non-controlled baseline emissions suggest significant effects. The base-case peak in this scenario is 139 ppb at 1700 in cell 31,22. **Table 12** summarizes the results corresponding to two climate-change scenarios.

Table 12. Simulated impacts with non-controlled emissions. Sacramento Valley, last day of episode.

	New peak at location and time of base-case peak (base=139 ppb)	New domain peak any time and location during last day	Largest increase anywhere in the domain
CCMA: GHG+S 2050	147 ppb (Δ = 8 ppb)	147 ppb (Δ = 8 ppb)	Δ = 12 ppb
CCMA: GHG+S 2090	149 ppb (Δ = 10 ppb)	149 ppb (Δ = 10 ppb)	Δ = 15 ppb

Thus the new peaks in Sacramento occur at the same location and time of the base-case peak. However, the largest increases in ozone occur at other locations and times. The 12-ppb increase occurs at 1600 in cell 30,21 (neighboring to location of base-case peak) whereas the 15-ppb increase occurs at 1500 in cell 29,21 and at 1600 in cell 30,21. These cells are adjacent to the location of the base-case peak.

Finally, **Table 13** shows a brief comparison of some aspects of simulated peak ozone with controlled (C) and non-controlled (NC) emissions.

Table 13. Comparison of peak and largest ozone changes for controlled and non-controlled emissions (all entries are in ppb).

			New peak at location and time of base-case peak				New peak anywhere in domain and anytime during last day of episode					
	Present-climate base-case peak ↓				Δ	Δ			Δ	Δ	Largest increase anywhere anytime	
CCMA cases ↓	C	NC	C	NC	C	NC	C	NC	C	NC	C	NC
Los Angeles	110	118										
GHG+S 2050			113	123	3	5	**113**	**127**	3	9	11	13
GHG+S 2090			114	130	4	12	**121**	**143**	11	25	26	31
Sacramento	120	139										
GHG+S 2050			128	147	8	8	**128**	**147**	8	8	10	12
GHG+S 2090			129	149	9	10	**129**	**149**	9	10	12	15

Column 2 is simply the present-climate base-case peaks for cases CCMA GHG+S. The columns labeled Δ show the difference from the corresponding (C or NC) base case, and the last column shows the largest increases in ozone concentrations anywhere in the modeling domains and anytime during the last day of the modeling episode. Note that the increases in ozone on the last day of the episode may be smaller than the increases during the first and second days of the episode (these days are not discussed in this report).

From **Table 13**, the following can be deducted: the change in peak ozone at the location and time of the base-case peak in the Los Angeles Basin is 1.6 times larger in case CCMA GHG+S 2050 NC compared to case CCMA GHG+S 2050 C. In year 2090, the ratio is almost three folds (2.8 times larger increases in peak ozone at location and time of base-case peak). In terms of new domain peaks (anywhere in domain) during the last day of the episode in Los Angeles, the effect of NC emissions is to increase the peak by 2.8 folds in 2050 and by 2.1 folds in 2090. The largest increases in ozone during the last day of the modeled episode are 1.2 times larger in cases NC than in cases C (for both 2050 and 2090).

For the Sacramento Valley, the following can be deducted: the changes in peak ozone at the location and time of the base-case peak and the changes in new domain peaks are relatively of the same magnitude for both cases NC and C and years 2050 and 2090. However, the largest increases in ozone during the last day of the modeled episode are 1.2 times larger in cases NC than in cases C (for both 2050 and 2090), which is similar to the results for the Los Angeles Basin.

The bottom line is that the effects of climate change on air quality are significant, with or without controlled emissions. The boldface numbers in the 4th column of Table 13 are perhaps the bottom line of this modeling study (as far as peak ozone is concerned). The future-year ozone peak concentrations (domain-wide) in **Los Angeles are 127 and 143 ppb** (for years 2050 and 2090, respectively) for non-controlled emissions. For controlled emissions, these numbers become 113 and 121 ppb. For **Sacramento**, the peak concentrations (domain-wide) are **147 and 149 ppb** (for years 2050 and 2090, respectively) for non-controlled emissions. With emission control, these numbers become 128 and 129 ppb.

5.4 Significance of predicted air quality impacts (controlled emissions only)

It is fairly difficult to choose a satisfactory "index" or basis for evaluating the significance of the climate-change impacts on ozone, reported in this study, relative to some other "known" impacts or effects. For one thing, there are many possible ways to interpret and re-cast the results, and also, some of these interpretations can be quite arbitrary and subjective.

Among the many possibilities, two comparisons are made here using only the **domain-peak** concentration changes as indicators. The first is to compare the air quality effects of climate change with the effects of switching from non-controlled to controlled emissions. The second is to "translate" the effects to equivalent emissions of ozone precursors, i.e., emissions of NOx and VOC.

Equivalence relative to controlled and non-controlled emissions:
As mentioned in Section 5.1, the air quality effect of controlled emissions (versus non-controlled emissions) on domain-peak concentrations was to decrease the simulated peak from about 118 down to 110 ppb (a change of 8 ppb) in the Los Angeles Basin and to decrease the domain peak from 139 to 120 ppb (a change of 19 ppb) in the Sacramento Valley. Note that these changes are heavily influenced by the assumed emission levels and controls and, thus, the numbers for Sacramento and Los Angeles cannot be compared directly. Also, the definition of controlled and non-controlled emissions is not necessarily the same as use by the air districts. By comparison, the effects of climate change on the domain peak (anywhere in domain) is to increase it by up to 11 ppb (**Table 3**) in the Los Angeles Basin and by up to 9 ppb (**Table 7**) in the Sacramento Valley. Thus on an order of magnitude, the effect of climate change is about equivalent to the effect of moving the regions from relatively non-controlled emissions to a case where committed controls are in place.

However, there may be a caveat in the basis of this comparison: it is difficult to accurately define what constitutes a controlled and non-controlled emissions scenario. That is, how much control should there be before a scenario can be labeled "controlled"? The same applies to non-controlled emissions. Obviously, the air districts should be consulted for a historical perspective on this definition and a more accurate assessment should be

done again in the future. But the caveat mentioned above can render this comparison, stronger, weaker, or flawed, at this time.

Equivalence relative to NOx and VOC emissions:
In previous modeling work, Taha et al. (2000) and Emery and Taha (2000) developed matrices of peak ozone concentrations versus various levels of emissions of NOx and VOC for the Los Angeles Basin and the Sacramento Valley. The matrices were constructed using the UAM itself. Based on these modeling results, it appears that for the Los Angeles Basin, a change of 4-11 ppb in the domain peak (from **Table 3**) is equivalent to a change of roughly 10% in non-controlled VOC and NOx emissions. In the Sacramento Valley, a change of 7-9 ppb in domain peak (from **Table 7**) is roughly equivalent to 15% reductions in non-controlled NOx and VOC emissions. Recall that there are larger changes in the domain than the changes in the peaks, and thus, would correspond to even larger equivalent NOx and/or VOC emission reductions. Although the correlations given here are crude and will need refining, they can still give an order-of-magnitude estimate for the relative potential implications of climate change.

6. MODEL PERFORMANCE EVALUATION

The UAM base-case model performance was evaluated for both the 1987 episode of the Los Angeles Basin and the 1990 episode of the Sacramento Valley (SCAQMD 1996, CARB 1995, Taha 1996,1997). In summary, the findings were that the UAM performance was satisfactory for both episodes and within model error tolerances set forth by the US EPA (EPA 1991).

7. ISSUES, CONCERNS, and RESEARCH NEEDS

As with any modeling study, there are issues, concerns, and caveats to keep in mind when evaluating the simulation results reported here. Some of these concerns relate to the assumptions made during the course of this study, e.g., those discussed in Section 3, whereas others are related to more fundamental issues, e.g., the model formulation, approximations, model performance, input data, and so on. It is known that the UAM-IV is now a relatively older-technology model, albeit still used. A more recent, state-of-science model should be used in future studies of this nature. In particular, models with more robust formulations and with process analysis capabilities would be more suitable. In addition, there are always uncertainties associated with emission inventories, such as those used here.

In addition to these generic concerns, the following items are related to this study. In particular, the issue of downscaling the coarse GCM forecast to local (i.e., State) scale and finer resolutions (e.g., 2-5 km) would be needed if more accurate assessments of meteorological changes and their air quality impacts are sought. This more accurate approach was not followed in this study. Some other concerns are:

A. In this modeling study, it is assumed that all areas within a modeling region are equally affected by meteorological changes, with no differentiation between urban and non-urban areas. While this may be justified, since the GCM grid is relatively coarse, it should be improved upon in the future by providing finer-resolution meteorological input to the photochemical model, through GCM downscaling (e.g., Giorgi et al. 1993a,b), as discussed earlier.
B. Urban heat islands are not "grown" in future-year scenarios. If the changes in heat island intensity and/or aerial extent are forecast to be significantly different in the future, this effect should be considered in addition to those of the background change in climate. The local effects of heat islands can sometimes be comparable to those induced by climate change.
C. The local population is not grown in future-year scenarios. A better accounting for the effects of population-related expansion in emission sources (geographical extent) and level of emissions should be accounted for in future modeling work of this type.
D. The spatial and temporal changes in air temperature, mixing heights, and emissions of isoprene were mapped and modified according to methods described in this report. A more accurate approach (which was beyond the scope and level of effort in this project) would, stated again, be to downscale the GCM output using mesoscale meteorological models and fine-tune the input to air quality models and emission processors accordingly. This approach should provide significant improvements in the accuracy of the air quality modeling forecasts since the meteorological changes will be provided to the photochemical model at finer spatial and temporal resolutions. This will also resolve many of the simplifying assumptions made in this study, i.e., those discussed in Section 3.
E. The results reported here are episode-and domain-specific and may not be of much value in generalizing or extrapolating the findings to other times, seasons, or geographical regions. Further modeling and analysis will be needed to cover these other areas and aspects of possible interest.

8. CONCLUSIONS

This preliminary modeling study addressed the potential ozone air quality implications of selected climate-change scenarios in California. The focus was on the effects of changes in temperature and some related meteorological and emission parameters. Two Californian regions were simulated: the Los Angeles Basin and the Sacramento Valley. In this study, the simulations were based on the air districts' representative modeling episodes and were performed using different versions of the Urban Airshed Model, as appropriate for each area. For both regions, future-year controlled emission inventories were used. In addition, limited simulations with non-controlled emissions were also performed in this study.

The episodic simulations suggest significant implications from potential climate change in California, even with controlled emissions. In the Los Angeles Basin, under controlled-emission scenarios, increases in ground-level ozone as large as 26 ppb could occur and in the Sacramento Valley, up to 12 ppb. At the locations *and* times of the domain base-case peaks, the increases are smaller but still significant. In the Los Angeles Basin, the domain peak can increase by up to 4 ppb and in the Sacramento Valley, by up to 9 ppb. The peak concentrations anywhere in the domain can increase by 11 ppb in the Los Angeles Basin and by up to 9 ppb in the Sacramento Valley. These changes are found to be significant if "translated" into NOx and VOC emission equivalents or compared to the effects of implementing committed controls in each of the two regions. The effects of using non-controlled emissions in the simulations are even larger. Using non-controlled emissions, ozone increases as large as 31 ppb can occur in the Los Angeles Basin and the peak (at location and time of base-case peak) increases by up to 12 ppb. Peak concentrations anywhere in the domain (new peaks) increase by up to 25 ppb. In the Sacramento Valley, the non-controlled emissions result in largest increases of up to 15 ppb anywhere in the domain and the peak (at location and time of base-case peak) increases by up to 10 ppb.

The climate change scenarios simulated in this study would bring both the Los Angeles Basin and the Sacramento Valley out of compliance. In addition, the total area-weighted times (hours) with exceedance concentrations more than double. The modeling results suggest that the changes in ozone concentrations in the Los Angeles Basin are in the range of 0.7-4.6 ppb/K (subject to restrictions). In the Sacramento Valley, the slopes are in the range of about 1.4-2 ppb/K (subject to restrictions discussed in the report). The slopes obtained from this study's simulations are relatively smaller than those from previous modeling studies by Taha and co-workers or those reported in past EPA literature, for example, for reasons discussed in the text. The slopes obtained from simulation scenarios with non-controlled emissions are, of course, larger.

The results presented in this report are episode- and region-specific and, thus, may not provide a suitable basis for generalization to other time periods, historical trends, or different regions. However, they still suggest that the potential role of climate change on ozone air quality in California can be significant and needs to be investigated further.

9. REFERENCES

Benkely, C.W. and Schulman, L.L., 1979. "Estimating hourly mixing depths from historical meteorological data", *Journal of Applied Meteorology*, Vol. 18 (June 1979), pp. 772-780.

California Air Resource Board (CARB) 1995. "Sacramento Area Modeling Analysis for the 1994 State Implementation Plan", Control Strategy Modeling Section, California Air Resource Board, Sacramento, California.

Emery, C. and Taha, H. 2000. "Reconciliation of two modeling efforts that estimate the air quality benefits of cool communities strategies in the South Coast Air Basin". Technical report prepared for the City of Los Angeles, Department of Environmental Affairs (July 2000). ENVIRON, Novato, California.

EPA 1988. "The potential effects of global climate change on the United States", Volume 2: National Studies. Draft Report to Congress, USEPA, October 1988.

EPA 1991. "Guideline for regulatory application of the Urban Airshed Model". EPA-450/4-91-013, Office of Air Quality Planning and Standards, Research Triangle Park, NC 27711.

EPA 1996. "Air quality criteria for ozone and related photochemical oxidants", Report EPA/600/P-93/0044aF (July 1996), National Center for Environmental Assessment, Office of Research and Development, USEAP, Research Triangle Park, NC 27711.

Giorgi, F., Marinucci, M.R., and Bates, G.T. 1993a. "Development of a second-generation regional climate model (RegCM2): Part I: boundary-layer and radiative transfer process". Monthly Weather Review, No. 121, pp. 2794-2813.

Giorgi, F., Marinucci, M.R., Bates, G.T., and De Canio, G., 1993b. "Development of a second-generation regional climate model (RegCM2): Convective processes and assimilation of lateral boundary". Monthly Weather Review, No. 121, pp. 2814-2832.

Guenther, A., Zimmerman, P. Harley, P., Monson, R., and Fall, R. 1993. "Isoprene and monoterpene emission rate variability: Model evaluations and sensitivity analysis", Journal of Geophysical Research, Volume 98, pp. 12609-12617.

Sillman, S. and Samson, P.J. 1995. "Impact of temperature on oxidant photochemistry in urban, polluted rural, and remote environments", Journal of Geophysical Research, Vol. 100, pp. 11497-11508 (1995).

Sillman, S., Logan, J.A., and Wofsy, S.C. 1990. "The sensitivity of ozone to nitrogen oxides and hydrocarbons in regional ozone episodes", Journal of Geophysical Research, Vol. 95, pp. 1837-1851, (1990).

South Coast Air Quality Management District (SCAQMD) 1996. "Proposed modification to the draft 1997 Air Quality Management Plan", October 1996, South Coast Air Quality Management District, Diamond Bar, California.

Taha, H. 1996. "Modeling the impacts of increased urban vegetation on the ozone air quality in the South Coast Air Basin", *Atmospheric Environment*, Vol. 30, No. 20, (1996), pp. 3423-3430.

Taha, H. 1997. "Modeling the impacts of large-scale albedo changes on ozone air quality in the South Coast Air basin, *Atmospheric Environment*, Vol. 31, No. 11 (1997), pp. 1667-1676.

Taha, H., Chang, S.C., and Akbari, H. 2000. "Meteorological and air quality impacts of heat island mitigation measures in three U.S. cities", LBNL Report 44222 (2000), Lawrence Berkeley National Laboratory, Berkeley, California 94720.

Taha, H. and Bornstein, R. 1999, "Urbanization of meteorological models: Implications on simulated heat islands and air quality", Invited paper, *International Congress of Biometeorology and International Conference on Urban Climatology*, 8-12 November, 1999, Sydney, Australia.

Taha, H., Douglas, S., and Haney, J. 1997. "Mesoscale meteorological and air quality impacts of increased urban albedo and vegetation", *Energy and Buildings, Special Issue on Urban Heat Islands*, Vol. 25, No. 2 (1997), pp. 169-177.

Taha, H., Liu, X., Sailor, D., Benjamin, M., Winer, A., Douglas, S., and Haney, J. 1994. "Analysis of energy efficiency and air quality in the South Coast Air Basin of California", Unpublished LBNL Report 35728 UC 000.

Trenberth, K.E. (ed.) 1992. Climate System Modeling. Cambridge University Press, pp.788.

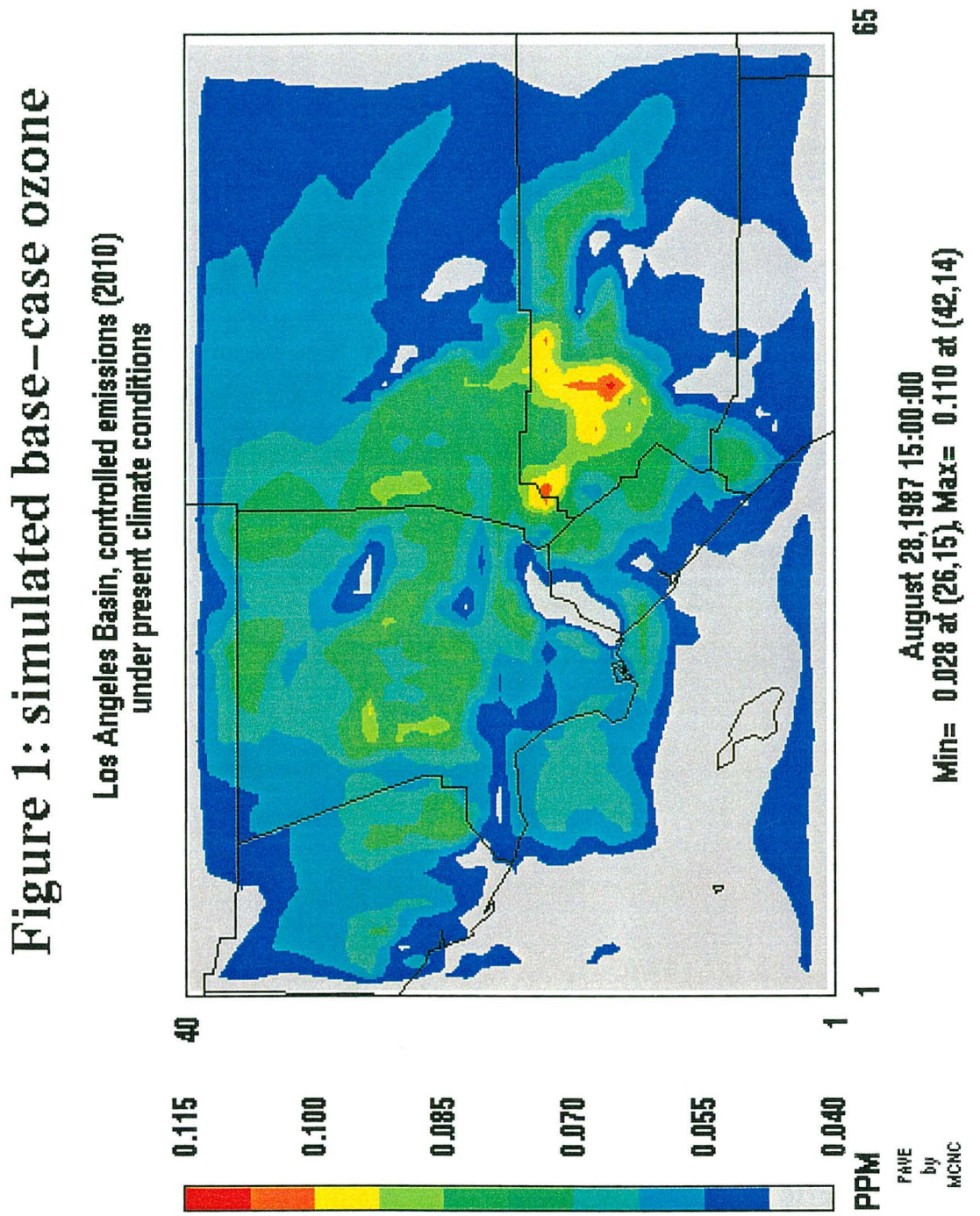

Figure 1: Simulated base-case ozone concentrations in the Los Angeles Basin under **current climate conditions** (year 2010 with controlled emissions). Peak base-case ozone concentration is 110 ppb at 1500 PDT on August 28.

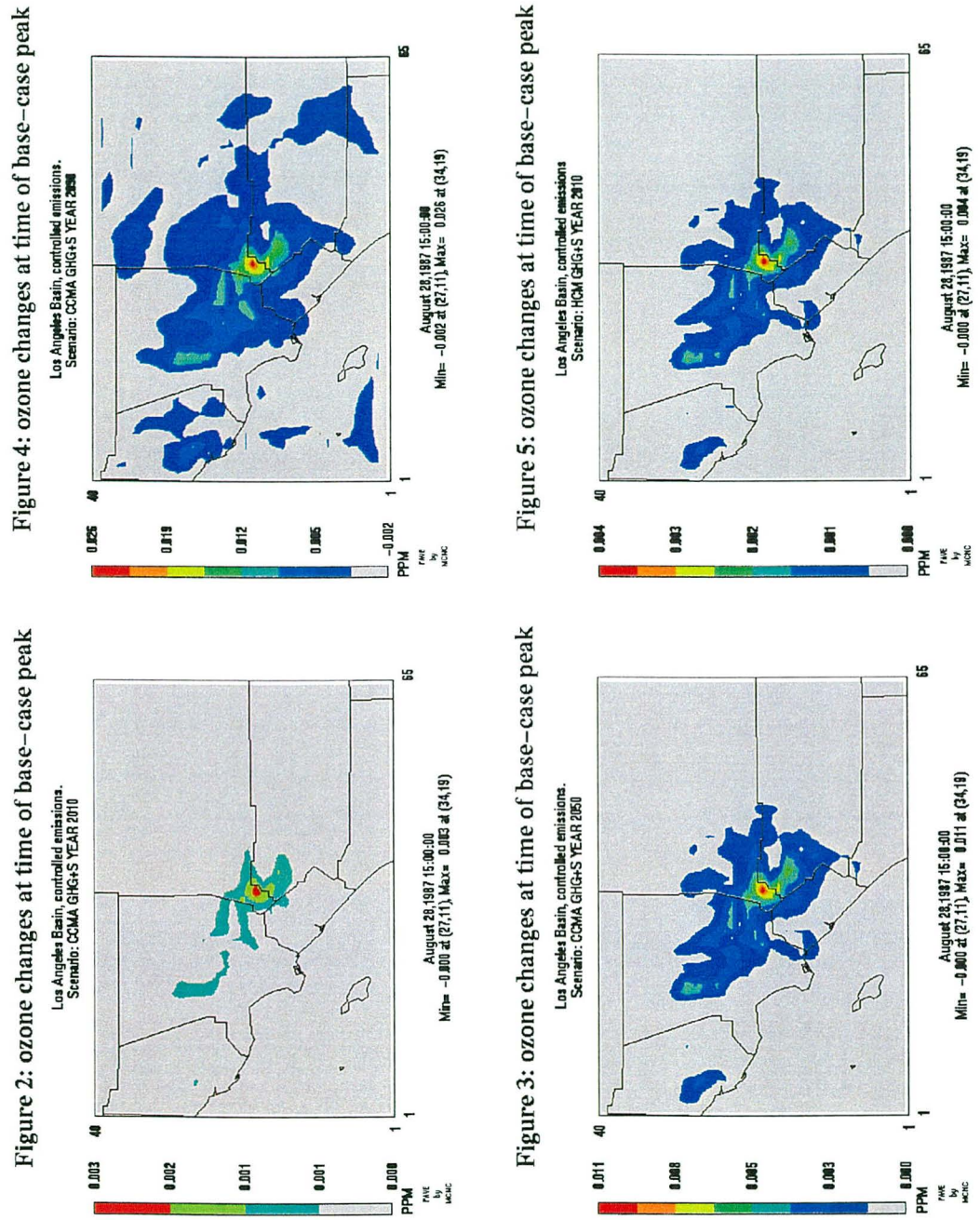

Figures 2,3,4, and 5. Difference in ozone concentrations at the time of base-case peak (1500 PDT, August 28) in the Los Angeles Basin, for cases CCMA year 2010 (**2**), CCMA year 2050 (**3**), CCMA year 2090 (**4**), and HCM year 2010 (**5**).

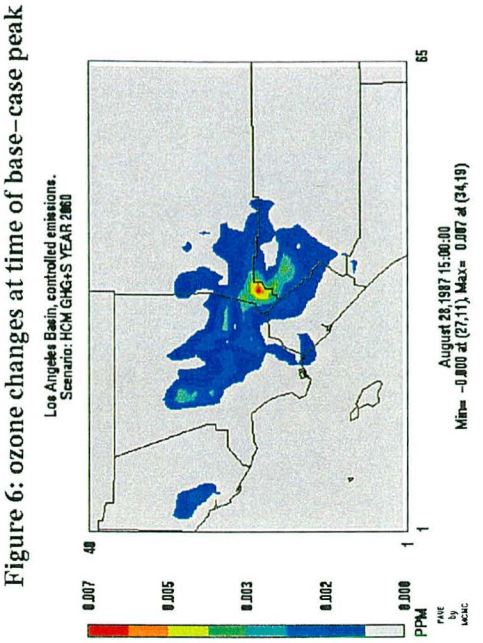

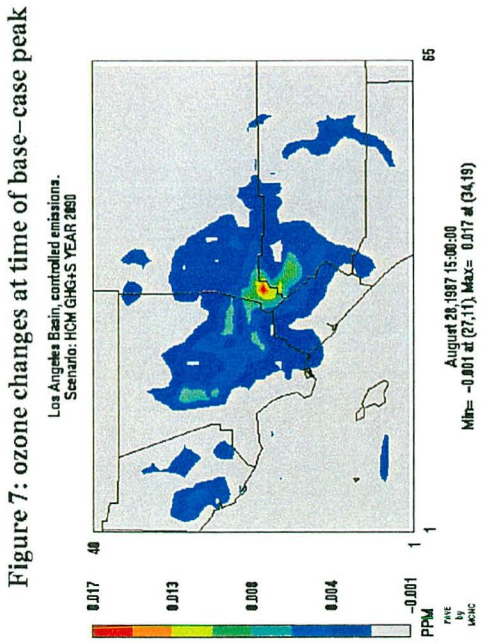

Figures 6 and 7. Difference in ozone concentrations at the time of base-case peak (1500 PDT, August 28) in the Los Angeles Basin, for cases HCM year 2050 (**6**) and HCM year 2090 (**7**).

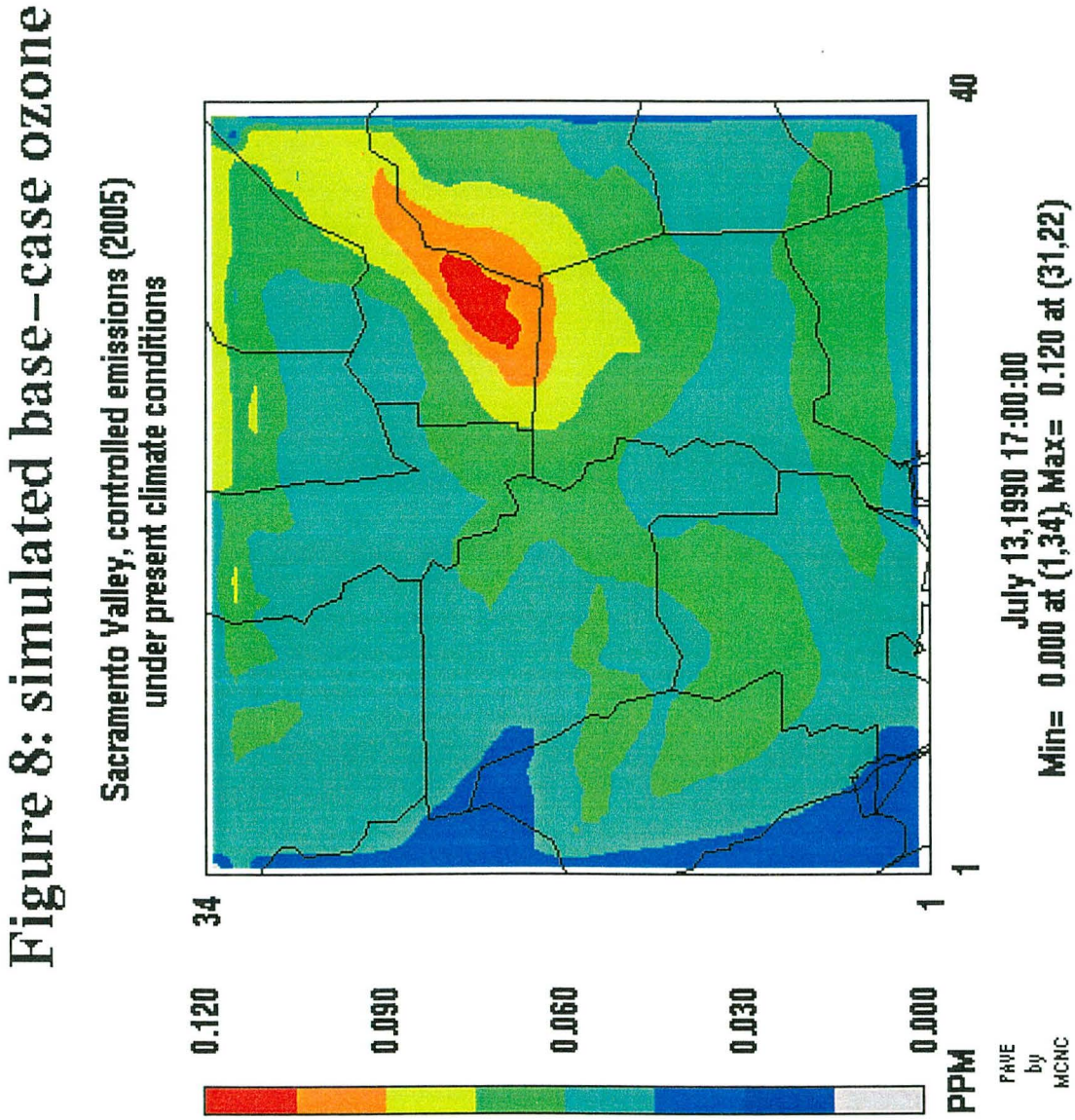

Figure 8: Simulated base-case ozone concentrations in the Sacramento Valley under **current climate conditions** (year 2005 with controlled emissions). The peak base-case ozone concentration is 120 ppb at 1700 PDT on July 13.

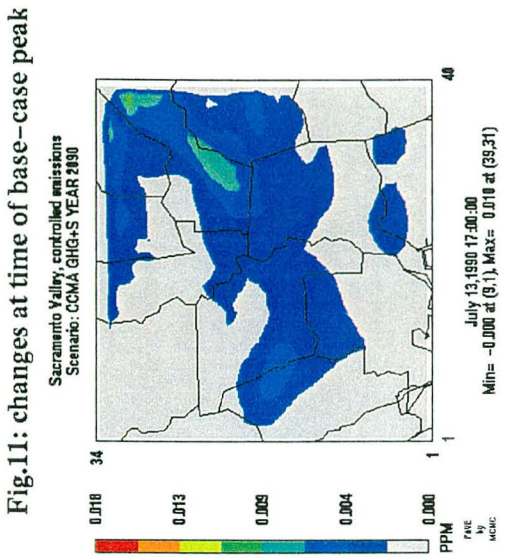

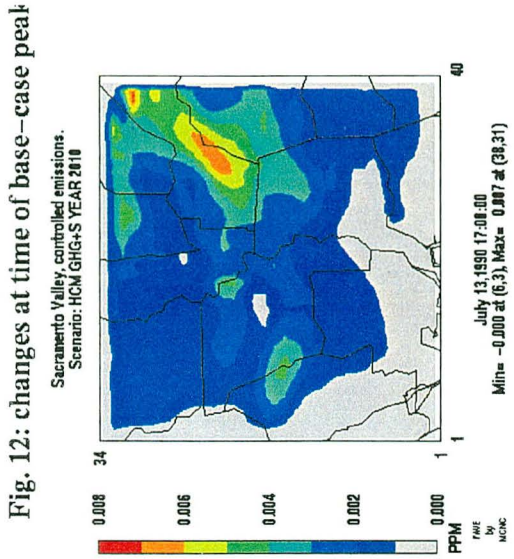

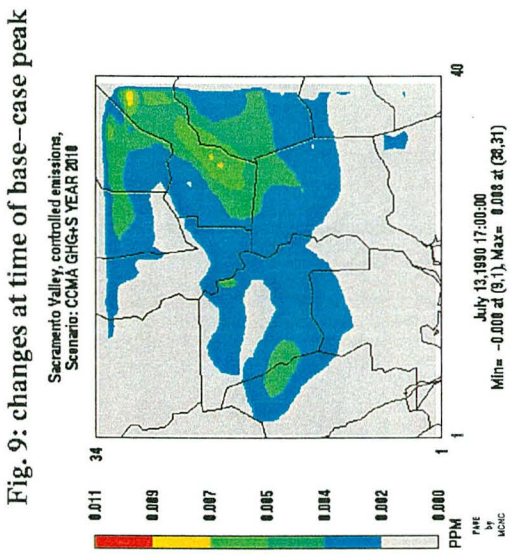

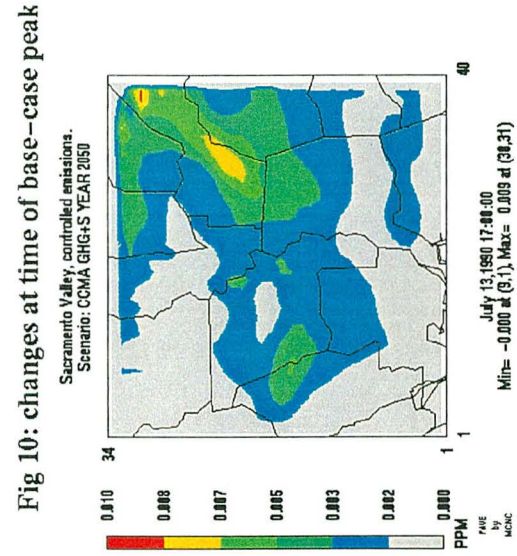

Figures 9,10,11, and 12. Difference in ozone concentrations at the time of base-case peak (1700 PDT, July 13) in the Sacramento Valley, for cases CCMA year 2010 (**9**), CCMA year 2050 (**10**), CCMA year 2090 (**11**), and HCM year 2010 (**12**).

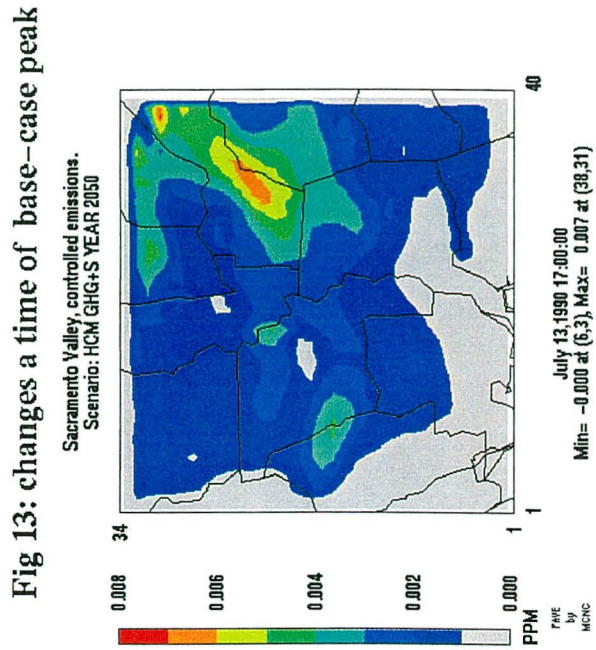

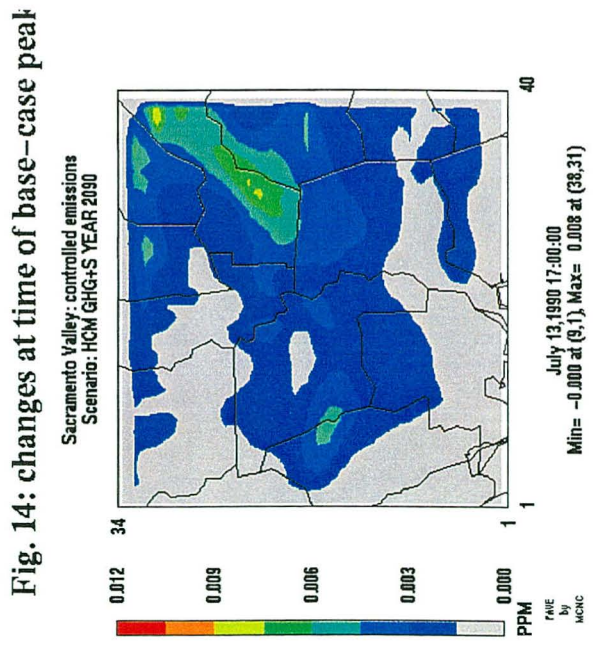

Figures 13 and 14. Difference in ozone concentrations at the time of base-case peak (1700 PDT, July 13) in the Sacramento Valley, for cases HCM year 2050 (**13**) and HCM year 2090 (**14**).

Ernest Orlando Lawrence Berkeley National Laboratory
One Cyclotron Road | Berkeley, California 94720

Prepared for the U.S. Department of Energy under Contract No. DE-AC03-76SF00098